Research Square

Preprints are preliminary reports that have not undergone peer review.
They should not be considered conclusive, used to inform clinical practice,
or referenced by the media as validated information.

Wheat peptides alleviate constipation by promoting enteric neurogenesis via mAChR-mediated calcium signaling pathways in mice

Qianqian Wang

wqq598223@zafu.edu.cn

Zhejiang A & F University

Fei Shen

Zhejiang University of Science & Technology

Guanghua He

Zhejiang University of Science & Technology

Juan Du

Hangzhou Kangyuan Food Science & Technology Co., Ltd.

Haiying Cai

Zhejiang University of Science & Technology

Minjie Zhao

Zhejiang University

Jing Wang

Zhejiang University

Haobin Zhao

Hangzhou Kangyuan Food Science & Technology Co., Ltd.

Lida Wang

Zhejiang Dermatology Hospital

Fengqin Feng

Zhejiang University

Article

Keywords: Wheat peptides, constipation, calcium signaling pathway, enteric neurogenesis, intestinal peristalsis

Posted Date: September 27th, 2024

DOI: https://doi.org/10.21203/rs.3.rs-4767421/v1

License: This work is licensed under a Creative Commons Attribution 4.0 International License.
Read Full License

Additional Declarations: (Not answered)

Wheat peptides alleviate constipation by promoting enteric neurogenesis via mAChR-mediated calcium signaling pathways in mice

Fei Shen[a, c, 1], Guanghua He[a, 1], Juan Du[f], Haiying Cai[a], Minjie Zhao[c], Jing Wang[c, d], Haobin Zhao[f], Lida Wang[g], Fengqin Feng[c, d, e], Qianqian Wang[b, c*]

[a] School of Biological and Chemical Engineering, Zhejiang University of Science & Technology, Hangzhou 310023, China

[b] College of Food and Health, Zhejiang A & F University, Hangzhou 311300, China

[c] College of Biosystems Engineering and Food Science, National-Local Joint Engineering Laboratory of Intelligent Food Technology and Equipment, Zhejiang Key Laboratory for Agro-Food Processing, Zhejiang University, Hangzhou, 310058, China

[d] Ningbo Research Institute, Zhejiang University, Ningbo, 315100, China

[e] ZhongYuan Institute, Zhejiang University, Zhengzhou, 450001, China

[f] Hangzhou Kangyuan Food Science & Technology Co., Ltd. Hangzhou 310012, China

[g] Doppler Ultrasonic Department, Zhejiang Dermatology Hospital, Huzhou 311203, China

[1] These authors contributed equally to the work

*Corresponding authors:

E-mail addresses: wqq598223@zafu.edu.cn

Tel/ Fax: +86-571-88982163

Abstract: Constipation is a prevalent gastrointestinal issue. Wheat peptides (WP) effectively alleviate loperamide-induced constipation in mice. Oral administration of WP (0.5 mg/g.bw) improved defecation, small intestinal propulsion, and intestinal barrier function in mice. WP also modulated gut inflammation and enteric nervous system factors. Additionally, WP intervention effectively rectified gut microbiota dysbiosis by restoring microbial diversity and modulating gut bacteria to approach normal levels. Of particular significance, transcriptome data indicated alterations in gene expressions related to the calcium signaling pathway in the colon of constipated mice. RT-qPCR analysis further corroborated that WP upregulated the gene expression of cholinergic receptor (*Chrm1*), *Itpr2*/*3*, *Calml3*, and Calm*4*. Furthermore, 3D microscopy revealed that WP increased the number of enteric nerves in the colon of constipated mice. These findings suggest WP mitigate constipation by activating muscarinic acetylcholine receptors, enhancing calcium signaling, and promoting enteric neurogenesis to improve intestinal peristalsis. Overall, WP demonstrate therapeutic potential for treating constipation.

Keywords: Wheat peptides, constipation, calcium signaling pathway, enteric neurogenesis, intestinal peristalsis

1. Introduction

Constipation, a prevalent gastrointestinal (GI) disorder, which was characterized by difficulties in defecation, reduced bowel movement frequency, prolonged GI emptying time and dry and firm feces in individuals [1]. This condition poses significant health risks and can have a detrimental impact on a patient's daily life, leading to psychological stress [2]. Nevertheless, satisfactory strategies for treating constipation remain elusive, as currently available options are associated with severe side effects such as strong drug dependence, high recurrence rates, and limited long-term effectiveness [3]. Therefore, there is an urgent requirement to develop secure and efficient drugs for the treatment of constipation. Natural bioactive substances (NBS) have gained popularity among consumers as they offer the advantages of low toxicity and fewer adverse effects [4].

The current research on relieving constipation in NBS including dietary fiber [5], saccharides [6], and probiotics [7], which can promote the gut motility. The enteric nervous system (ENS) intricately regulates gut motility through its intramural reflex pathways. Comprised of numerous discrete small ganglia that maintain neural continuity, the ENS forms two distinct ganglionated neuronal plexuses known as the myenteric and submucosal plexuses [8]. Generally, the myenteric plexus coordinates the muscle movements involved in content propulsion, while the submucosal plexus is primarily associated with secretion and absorption [8]. Several studies have indicated that the positive effects of NBS on gut motility are mediated by the nervous system, providing evidence for the potential of NBS to regulate the ENS and normalize gut motility [9].

We previously reported that wheat peptides (WP) were potential functional food in alleviating constipation in human and mice at the dose of 2 mg/g by enhancing

water-electrolyte metabolism, accelerating intestinal motility, and remodeling intestinal microbiota [10]. A subsequent trial of our team demonstrated that 1mg/g of WP with different hydrolysis degree was also efficacious at reliving constipation in constipated mice [11]. However, the potential targets of WP on alleviating constipation had yet to be investigated. For another, based on patients' choice of different doses from mild to severe symptoms, and whether constipation relief could be achieved at a lower cost (means lower dose). With the advancement of high-throughput sequencing, RNA-seq analysis has proved its effectiveness in investigating potential molecular mechanism, and have been largely applied in disease studies. Thus, employing RA-seq could give us a deeper insight into the underlying mechanisms accountable for the constipation-relieving effects of WP.

Consequently, this study intends to assess the therapeutic value of WP at a minor amount of 0.5 mg/g in ameliorating Lop-induced constipation in mice. The evaluation will involve measuring key constipation indicators, such as fecal elimination parameters and gastrointestinal motility rate. Furthermore, the study aims to elucidate the underlying mechanism of WP in alleviating constipation by analyzing colonic genome-wide transcriptional profiles. The goal is to gain new insights into the potential of WP as a preventive and therapeutic approach for constipation.

2. Material and methods

2.1. Materials

The WP was acquired from Hangzhou Kangyuan Food Science and Technology Co., Ltd., located in Hangzhou, China. The basic chemical composition of WP including moisture (3.91%), ash (3.54%), fat (2.47%), protein (80.05%), and carbohydrate (13.94%). WP was mainly composed of peptides below 5,000 Da,

accounting for 75.19% of peptides. In the WP, a total of 18 amino acids were detected, with a combined content of 76.66 g per 100 g. Among these amino acids, the top five in terms of concentration were glutamine (22.91g/100g), proline (9.92g/100g), leucine (5.43g/100g), glutamic acid (4.61g/100g), and phenylalanine (4.25g/100g). Loperamide (Lop), a pharmaceutical compound used for modeling purposes, was acquired from Xi'an Janssen Pharmaceutical Ltd. located in Xi'an, China. Activated carbon was purchased from Zhejiang Wanglin Biological Co. Ltd (Hangzhou, China). Arabic gum was sourced from National Drug Reagents Co., Ltd. (Beijing, China).

2.2. Animals and treatment

The animal experimental procedures were conducted in compliance with the regulations set forth by the Ethics Committee of Experimental Animals at Zhejiang Chinese Medical University (approval code: 20220425-28). Four mice per cage were housed in Zhejiang Chinese Medical University. All mice in a controlled environment (12 h daylight cycle) with chow (M2012, Fanbo Biotechnology Co., Ltd, China) and water ad libitum. After acclimation for 1 week, 36 male BALB/c mice (Shanghai SLAC Laboratory Animal Co., Ltd., China), weighing 20 ± 2g, were randomly assigned to three groups (n=12): the control group (CON), the constipation model induced by Loperamide group (LOP), and the group treated with wheat peptides (WP), with twelve mice in each group. Mice in both the LOP and WP groups were given Lop (10 mg/kg·bw) half an hour before the daily treatment, whereas the mice in the CON group received saline. The WP group was orally administered the corresponding dose of wheat peptides (0.5 mg/g.bw) daily, while the other two groups received daily saline treatment. Throughout the experiment, all mice were provided unrestricted access to water and standard feed. Body mass and food consumption were assessed every four days for each group. After 16 days, mice were fasted for 12 h, and fully

anesthetized through intraperitoneal injection of 2% pentobarbital sodium (Shanghai Aladdin Biochemical Technology Co., Ltd, Shanghai, China) at the dose of 40 mg/kg and then the mice of slaughter method were using cervical dislocation that complied with the EU Directive.

2.3. Assessment of fecal elimination function

2.3.1. Defecation test

The 6 h defecation experiment was carried out to detect the defecation status of mice [10]. On the 13th day, all mice underwent a 16-hour fasting period with access to water. The following morning, the LOP and WP groups received Loperamide (10 mg/kg·bw), whereas the CON group was administered saline. After thirty minutes, all mice were gavage-fed the activated carbon suspension (0.01 mL/g.bw). Each mouse was promptly moved to a fresh cage with unrestricted access to food and water. Key defecation indicators, such as the first black stool time, number of fecal pellets, dry feces weight, wet feces weight, and fecal water content were assessed.

2.3.2. Small intestinal motility test

The small intestinal motility test was carried out to detect the GI transit rate [12]. On the 16th day, all mice underwent a 16-hour fasting period with access to water. The following morning, the LOP and WP groups received Loperamide (7.5 mg/kg·bw), whereas the CON group was administered saline. After thirty minutes, all mice were gavage-fed the activated carbon suspension (0.01 mL/g.bw). After thirty minutes, the mice were euthanized, and the complete GI tract was removed. The GI transit rate was executed using the following formula:

$$\text{GI transit rate (\%)} \frac{\text{Length of intestinal propulsion of carbon}}{\text{Total length of small intestine}} \times 100$$

2.4. Histological analysis

The ileum and colon were placed in 4% paraformaldehyde solution immediately after dissection. The specimens were embedded in paraffin wax and subsequently cut into sections with a thickness of 5 μm. Subsequently, conventional hematoxylin and eosin (H&E) staining was conducted. Randomly selected slides of the ileum and colon samples were observed under a microscope (Leica, Germany) at magnifications of 4× and 10×, respectively. Quantitative analysis of the villi height and crypt depth was performed using Image Pro 6.0 software (Media Cybernetics, USA).

2.5. Serum and colon biochemical analysis

The levels of serum lipopolysaccharide (LPS), somatostatin (SS), endothelin-1 (ET-1), substance P (SP), and motilin (MTL) were measured in 50 μL of mouse serum using ELISA kits (Jiyinmei, Wuhan, China) following the manufacturer's instructions. For the determination of interleukin 10 (IL-10) and tumor necrosis factor-alpha (TNF-α), approximately 60 mg of colon tissue was weighed and mixed with pre-cooled normal saline in a 1:9 ratio. After homogenization, the mixture was centrifuged at 12,000 g (4 °C) for 15 minutes. The resulting homogenate was utilized for the determination of TNF-α and IL-10 using the corresponding ELISA kit (Jiyinmei, Wuhan, China).

2.6. Real-time PCR quantification

Total RNA of colon tissues was extracted utilizing Invitrogen TRIzol solution (CA, USA). The extracted RNA, at the same concentration, was converted into complementary DNA (cDNA) with the Vazyme HiScript III RT SuperMix Kit (Nanjing, China). The RT-qPCR protocol followed the previously reported method (Zhong et al., 2020). The quantitative PCR (qPCR) analysis was conducted utilizing the ChamQ™ SYBR® Color qPCR Master Mix (Vazyme Corp., Nanjing, China) and LC480 Real-Time PCR system (Roche Diagnostics, Penzberg, Germany). The

following conditions were used: 95 ℃ for 30 s, followed by 40 cycles of 10s at 95℃ and 30s at 60℃, 95 ℃ for 15 s, 60 ℃ for 60 s, and 95 ℃ for 15 s. To quantify the variances in transcript levels, normalization of each amplicon to GAPDH was performed, and the relative gene expression was determined using the $2^{-\Delta\Delta Ct}$ method. All primer sequences here were generated by Zhejiang Sunya Biotechnology Co., Ltd. (Hangzhou, China) (Table S1).

2.7. 16S rDNA sequencing of gut microbiota

The 16S rRNA analysis protocol was performed to analyze the composition of gut microbiota [13]. Fecal samples from the CON, LOP, and WP groups (n = 6 per group) were collected on the 13th day. DNA extraction and purification were carried out using the TIANamp Stool DNA Kit (Beijing, China). The amplification of the V3-V4 region of the 16S rRNA gene was conducted using the universal primers F341 and R806.The resulting PCR products were then detected through agarose gel electrophoresis using a 2% gel. Subsequently, the PCR products were recovered and subjected to library testing. The library was quantified by Qubit, and then sequenced by computer (Illumina HiSeq PE250). The data was de-chimerized and clustered by Usearch (V10) software. In clustering, the sequence set with 97% similarity was regarded as operational taxonomic units (OTUs), and then compared and classified according to OTUs homology. The Reads of each sample was randomly flattened, and the corresponding OTUs sequence was extracted. The flattened OTUs was analyzed by QIIME software, and the representative sequence was compared with the 16S database, thus the species of each OTUs was classified. The species composition and differential bacteria were analyzed and plotted by QIIME2 and R3.6.3 software.

2.8. Transcriptome analysis

Transcriptomic analysis was performed using the procedure outlined by the previously reported method with minor modification [14]. Colon samples were subjected to total RNA extraction, and subsequently, paired-end reads were generated through sequencing on an Illumina Novaseq 6000 platform by Shanghai Major Biotechnology Co., Ltd. (Shanghai, China). The raw reads in Fastq format underwent processing using customized Perl scripts, which involved the removal of adaptor sequences and low-quality reads. All subsequent analyses were performed solely on data that was high-quality and free from contaminants. Gene expression levels were quantified using the Fragments Per Kilobase of transcript per Million mapped reads (FPKM) method. Differential expression analysis was conducted using the DESeq R package (version 1.10.1), and the resultant P-values were adjusted using the Benjamini-Hochberg (BH) method to manage the false discovery rate. We performed differential expression analysis to identify genes that were differentially expressed (DEGs). DEGs were identified using the criteria of $|\log2FoldChange| \geq 1.5$ and a corrected P-value < 0.05 in the comparisons of LOP *vs* CON and WP *vs* LOP.

2.9. Caecum SCFAs and BCFAs contents analysis

The cecal contents were analyzed to determine the levels of short-chain fatty acids (SCFAs), including acetate, propionate, and butyrate, as well as branched-chain fatty acids (BCFAs), which encompass isobutyrate, valerate, isovalerate, and caproate. Briefly, a fecal sample weighing 50 mg was homogenized with 250 μL of sterile distilled water for a duration of 5 minutes. Following that, the sample was supplemented with 10 μL of HCl and vortexed for 1 minute. It was subsequently allowed to equilibrate at room temperature for 5 minutes before undergoing centrifugation at 12,000 rpm (4 °C) for 20 min. After this, the liquid of upper layer (200 μL) was collected and 2-ethyl butyric acid (0.5 μL) was added as an internal

192 standard. Ultimately, the mixture was vortexed once more for 1 minute, then
193 centrifuged at 12,000 rpm (4 °C) for 5 minutes, and the resulting supernatant was
194 collected for GC analysis. Analysis of 1 μL of the injection solution was performed
195 using a Shimadzu GC-2014 capillary gas chromatograph, fitted with a DB-FFAP
196 column from J&W Scientific (Agilent Technologies, CA, USA).

197 *2.10. Three-dimensional imaging of the colonic nerve*

198 The protocol of 3D imaging was performed to detect the morphology of colonic
199 nerve [15]. Colon was fixed with 4% paraformaldehyde solution. Initially, the colon
200 tissue block was subjected to the Clear, Unobstructed Colon Imaging Cocktails and
201 Computational analysis (CUBIC) protocol for clearing purposes. In brief, the
202 paraformaldehyde-fixed colon tissue was resected into tissue blocks, followed by
203 wash with PBS. The tissue blocks were soaked in 8-10 ml of 50% ScaleCUBIC-1
204 reagent (a 1:1 mixture of water and CUBIC-1) for one day, followed by immersion in
205 8-10 ml of pure CUBIC-1 reagent for three days. Following that, the samples
206 underwent PBS washing and were then submerged in 8-10 ml of 50% ScaleCUBIC-2
207 reagent (a 1:1 mixture of water and CUBIC-2) for one day, followed by immersion in
208 8-10 ml of pure CUBIC-2 reagent for two days. We then performed immunostaining
209 with tubulin beta 3 (neuronal marker), incubated at room temperature for 3 days.
210 Finally, the incubated colon tissue was imaged using a Nuohai LS18 tiling light sheet
211 microscopy (Bitplane, Imaris 9.0).

212 *2.11. Statistical Analysis*

213 The gathered data underwent thorough statistical analysis to assess the significance
214 of the observed findings. All statistical analyses were performed using GraphPad
215 Prism 6.0 software. To assess the differences between groups, an analysis of variance
216 (One-way ANOVA) was performed for continuous variables, followed by Tukey's

test for the analysis. The data are expressed as means ± SEM, and statistical significance was determined at a *P*-value < 0.05.

3. Results

3.1. WP could relieve Lop-induced constipation in mice

As illustrated in Fig. 1, the LOP group showed reduced body weight gain in comparison to the CON group ($P < 0.001$), with the WP group reversing this trend (Fig. 1B). However, there were no notable differences in energy intake observed among the groups ($P > 0.05$, Fig. 1C). In terms of fecal parameters, the LOP group exhibited a significantly longer duration to excrete the initial black stool ($P < 0.0001$, Fig. 1D). Additionally, the LOP group exhibited a reduction in the quantity of fecal particles, stool wet weight, water content, and GI transit compared to the CON group ($P < 0.05$, Fig. 1E, 1G-I). Conversely, treatment with a low dose of WP (0.5 mg/g.bw) reversed these parameters, except for fecal water content ($P < 0.05$). Compared to the LOP group, The WP group exhibited a significantly shortened time taken for the first black fecal excretion by 22.1% ($P < 0.01$, Fig. 1D). The number of fecal pellets in the WP group increased by 20.1% ($P < 0.05$, Fig. 1E). Moreover, WP intervention markedly expedited the rate of small intestine transit in constipated mice by 37.5% ($P < 0.01$, Figure 1I). These results indicate that WP effectively alleviated Lop-induced constipation.

3.2. WP promoted the restoration of the mechanical barrier in constipated mice

H&E staining was implemented to determine the structural variation of the colon and small intestine tissues (Fig. 2A-D). In the LOP group, the ileum tissue displayed destroyed and shortened villi in contrast to the CON group. Nevertheless, WP treatment restored the villi and crypt to a normal level, which was not significantly

varied in comparison with the CON group ($P > 0.05$, Fig. 2A-D). Additionally, the thickness of the colonic muscle layer was reduced in the LOP group compared to the CON group. Following WP intervention, the colonic muscle layer thickened (Fig. 2A).

Claudin-1, Occludin, and Zo-1 play a vital role in maintaining the integrity of tight junctions in the intestinal barrier. In our research, the levels of *Claudin-1* and *Zo-1* expression in the colon were notably diminished in the LOP group in comparison to the CON group ($P < 0.05$, Fig. 2E). Nonetheless, administration of WP substantially enhanced the levels of *Claudin-1* and *Zo-1* expression ($P < 0.05$, Fig. 2E). Unfortunately, WP did not have a significant repair effect on mucosal barrier proteins mucin 2 (*Muc2)* and mucin 3 (*Muc3)* ($P > 0.05$, Fig. 2E). Nevertheless, these outcomes imply that WP effectively repairs the intestinal mechanical barrier in mice with constipation.

3.3. WP affected the level of inflammatory factors in constipated mice

Based on the histological findings, constipation appeared to induce colon tissue inflammation. Consequently, we quantified the amounts of cytokines connected to colonic inflammation. As shown in Fig. 2F-H, the levels of LPS and TNF-α were significantly higher in the LOP group compared to the CON group ($P < 0.05$, Fig. 2F-G). These findings suggest the presence of intestinal inflammation resulting from constipation. Treatment with WP decreased but not significantly the level of colonic TNF-α ($P > 0.05$, Fig. 2G). However, the IL-10 levels exhibited a significant decrease in the LOP group compared to the CON group ($P < 0.05$), but following WP treatment, they reverted to a non-significant difference from the CON group ($P > 0.05$, Fig. 2H). These findings suggest that WP exhibits an anti-inflammatory effect in constipated mice.

3.4. WP improved the smooth muscle pacing in constipated mice

Cajal's interstitial cells (ICC), known as slow-wave pacemaker cells in the GI tract, play a crucial role in intestinal motility [16]. The proteins receptor tyrosine kinase (c-Kit) and its ligand stem cell factor (SCF) serve as markers for ICC. The LOP group exhibited a significant down-regulation in the gene expression of *c-Kit* and *SCF* compared to the CON group ($P < 0.0001$, $P < 0.05$, Fig. 2I-J). However, administration of WP resulted in a significant up-regulation of *c-Kit* and *SCF* expression when compared to the LOP group ($P < 0.0001$, $P < 0.05$, Fig. 2I-J). These findings imply that WP enhances smooth muscle pacing, leading to accelerated intestinal motility.

3.5. WP balanced the secretion of enteric nervous factor in constipated mice

The enteric nervous factors (MTL, SS, ET-1, and SP) were determined to evaluate the intervention effect in constipated mice. WP treatment in constipated mice led to a significant increase in MTL and SP levels ($P < 0.01$) compared to the MC group, while SS and ET-1 levels were significantly reduced ($P < 0.05$) (Fig. 2K-N). WP treatment in constipated mice helped restore the equilibrium of enteric nervous factors secretion, as indicated by the aforementioned indexes.

3.6. WP remolded gut microbial structure in constipated mice

In totally, 736 OTUs were identified across the CON, LOP, and WP groups. The WP group had the highest number of detected OTUs (674), while the LOP group had the lowest (620) (Fig. 3E). WP treatment increased α-diversity compared to the LOP group, as indicated by the Shannon diversity parameter, which reached a level similar to that of the CON group ($P < 0.05$, Fig. 3A). Nevertheless, there were no notable variations among the groups in terms of Chao 1, Ace, and Simpson diversity indices ($P > 0.05$, Fig. 3B-D). Non-metric multidimensional scaling analysis (NMDS) was

employed to assess the structural changes, divergence, and community composition (β-diversity) of the gut flora in each group. The clusters of gut microbiota in LOP and CON groups showed some degree of separation, with the WP group cluster positioned between the CON and LOP groups (Fig. 3F).

Analysis based on taxa offers insights into the structural composition of the groups. On the phylum level, *Bacteroidota*, *Firmicutes*, *Campilobacterota*, *Desulfobacteria*, and *Patescibacteria* were consistently present across all groups (Fig. 3G). Notably, WP treatment reduced the proportion of *Firmicutes* and elevated the proportion of *Bacteroidetes* in Lop-induced mice. To further assess the regulatory impact of WP on the genus-level composition of gut bacteria, a heatmap analysis was conducted. The relative amounts of 30 significantly different genera were displayed among the three groups. As depicted in Fig. 3H, a significant portion of the observed alterations in the LOP group were statistically inhibited after WP treatment.

In order to delve deeper into the influence of WP on the microbiota of constipated mice, we performed LEfSe analysis to identify distinctive flora within each group (Fig. 4A). The prevailing bacteria in the WP group were *Jeotgalicoccus*, *Turicibacter*, *Oscillospiraceae*, and *Enterococcus*, whereas *Peptococcaceae* and *Oscillospirales* were dominant in the CON group. The function and characteristic genera of each group were analyzed separately based on the LEfSe results (Fig. 4C-F). The relative abundance of the *Bifidobacterium*, *Jeotgalicoccus*, and *Turicibacter* genera showed notable increasing trends in the WP group compared to the LOP group ($P < 0.0001$, Fig. 4C-E). Interestingly, following WP intervention, the relative abundance of *Helicobacter*, a well-studied harmful genus in digestive disease research, significantly reduced relative to the LOP group ($P < 0.001$, Fig. 4F).

To explore the potential correlation between changes in intestinal microflora induced by WP and environmental factors, we conducted correlation analysis using the Spearman method (Fig. 4B). The results revealed several significant correlations. The enrichment of *Jeotgalicoccus* in the WP group was positively correlated with *ZO-1*, *Claudin-1*, *c-Kit*, *SCF*, GI function, and IL-10 levels. Additionally, the enrichment of *Turicibacter* in the WP group displayed a significant positive association with *c-Kit* and *SCF* ($P < 0.01$, Fig. 4B). On the other hand, the *Helicobacter* genus exhibited significant positive and negative correlations with the first black stool time (FBST) and GI transit rate ($P < 0.05$, Fig. 4B).

3.7. WP altered the caeca SCFAs and BCFAs profile in constipated mice

Fig.5A-I illustrates the impact of WP on SCFAs and BCFAs in the ceca of Lop-induced mice. Contrasted with the LOP group, WP significantly enhanced the total content of SCFAs (Fig. 5D) and decreased the total content of BCFAs (Fig. 5I) ($P < 0.05$). Specifically, the propionate and butyrate levels were noticeably raised in the WP group (Fig. 5B and 5C) ($P < 0.05$), while isobutyrate, valerate, and caproate levels exhibited significant downregulation in the WP group (Fig. 5E, 5F, and 5H) ($P < 0.05$).

3.8. Effect of WP intervention on colonic gene expression utilizing transcriptome analysis in constipated mice

Examining alterations in gene expression in response to external stimuli is effectively facilitated through transcriptome analysis. In this research, we conducted transcriptome analysis to investigate the changes in colonic gene expression on a genome-wide scale. The volcano plots in Fig. 6A and 6B depict the differentially expressed genes (DEGs) between two groups (LOP vs. CON and WP vs. LOP, respectively). In comparison to the CON group, the LOP group exhibited 160

up-regulated DEGs and 409 down-regulated DEGs. Conversely, in the WP group, there were 197 differentially upregulated genes (DEGs) and 219 differentially downregulated genes (DEGs) in comparison to the LOP group (Fig. 6D). The heatmap analysis revealed that most of the DEGs in the Lop-induced group were reversed to resemble the CON group following WP treatment. For KEGG enrichment analysis, we selected the 20 most significant signaling pathways ($P < 0.05$). Among them, the calcium signaling pathways were found to be associated with intestinal motility. Table S2 summarizes the DEGs that were reversed by WP intervention in calcium signaling pathways. To validate the transcriptome sequencing-derived gene expression patterns, RT-qPCR analysis was performed on seven genes listed in Table S2. The results (Fig. 7C) indicated that the expression profiles of these genes were in line with those obtained from the transcriptome sequencing (Table S2). Relative to the LOP group, WP intervention up-regulated the expression of cholinergic receptor genes, including muscarinic acetylcholine receptor M1 (*Chrm1*, belonging to mAChRs), as well as inositol 1,4,5-triphosphate receptor 2/3 (Itpr2/3), calmodulin 4 (*Calm4*), and calmodulin-like 3 (*Calml3*), and solute carrier family 8 (sodium/calcium exchanger), member 3 (*Slc8a3*) (Fig. 7C). These genes are associated with the calcium signaling pathway, suggesting that WP has the ability to up-regulate this pathway. Muscarinic acetylcholine receptor M1 is activated by Ach, so we measured the content of Ach in serum (Fig. 7B). The serum Ach significantly decreased in LOP group compared with CON group ($P < 0.05$), while the intervention of WP significantly upregulated Ach ($P < 0.05$). This result further proved that WP could up-regulate Ach activation of calcium signaling pathway and relieve constipation.

3.9. WP promoted the recovery of colonic nerves in constipated mice

Fig. 7D displays images of the colonic nerves. In the CON group, the nerves appeared dense and clear. However, capturing nerve images became challenging under the same antibody fluorescent staining conditions after Lop modeling. The LOP group exhibited a decreased number of observed nerves. Following WP intervention, although the number of enteric nerves did not fully recover to the level observed in the CON group, it was significantly greater than in the LOP group. This indicates that WP has the potential to partially restore the reduction in the number of enteric nerves caused by Lop modeling.

4. Discussion

In a previous study, it was demonstrated that WP efficiently alleviated constipation in mice at doses of 2 mg/g and 1 mg/g [11, 10]. At these doses, WP significantly shortened the time of the first black stool excretion, elevated the number of fecal pallets with 5 hours, and improved fecal moisture content. In this current study, even at a reduced dosage of 0.5 mg/g in mice, WP continued to alleviate constipation by shortening the first black stool defecation time, increasing intestinal propulsion rate, and increasing the number of fecal pallets in 5 hours. However, unlike the higher doses of 2 mg/g and 1 mg/g, the fecal moisture content was not significantly restored at 0.5 mg/g. This suggests that WP may employ alternative mechanisms to relieve constipation, distinct from simply increasing water content in the stool to lubricate the intestines.

Constipation is frequently accompanied by intestinal tissue injury, compromised gut barrier integrity, and mild intestinal inflammation. In this study, we observed these abnormal symptoms, including alterations in intestinal villi morphology, colon wall thickness, tight junction proteins (Claudin-1 and ZO-1), proinflammatory factor

(TNF-α), and the inflammatory cytokine IL-10 in constipated mice. However, these symptoms were significantly improved following treatment with WP (Fig. 2). These findings align with a study conducted by Zhang et al. [17], who reported that Chitosan oligosaccharides could attenuate inflammatory responses and protect against intestinal barrier dysfunction in constipated mice induced by Lop [17]. The advantageous effects of WP may be ascribed to its high content of glutamine (Gln). Deprivation of Gln has been demonstrated to influence intestinal tight junctions through the PI3-K/Akt mediated pathway in Caco-2 cells [18]. Additionally, pretreatment of Caco-2 cells with Gln has been found to mitigate the decline in the expression of tight junction proteins, such as ZO-1 and Occludin [19]. In terms of inflammation, research in humans has provided evidence for the role of Gln in boosting levels of IL-10 (the anti-inflammatory cytokine) in the GI tract [20, 21].

Constipation's pathogenesis has been linked to the gut microbiota [22, 23]. Nevertheless, it remains uncertain whether the imbalance of gut microbiota causes Lop-induced constipation or if the microbiota imbalance is simply a consequence of constipation. Nonetheless, we observed changes in the intestinal bacteria between the LOP and CON groups, suggesting a relationship. These changes were evident at the levels of α-diversity (Shannon diversity parameter), β-diversity, as well as phylum and genus composition. Interestingly, WP intervention reversed these changes towards the pattern observed in the CON group, indicating its ability to promote a more homeostatic gut flora. In this study, the abundances of *Bifidobacterium*, which has been extensively studied for its potential to relieve constipation [24], were significantly increased by WP intervention. The role of *Turicibacter* in constipation is somewhat controversial. Lu et al. reported a positive correlation between *Turicibacter* and defecation frequency [25]. However, Chai et al. found no significant correlation

between *Turicibacter* and faecal dryness or colonic motility [24]. Interestingly, the *Turicibacter* was significantly increased with WP intervention in this study, whereas it decreased in our previous study with WP. On one hand, an enrichment of *Turicibacter* abundance may persistently disturb neurotransmitter system balance by hindering the 5-HT system, which can affect intestinal motility. On the other hand, *Turicibacter* is associated with intestinal butyrate production, which can enhance the intestinal barrier and exert anti-inflammatory effects. In our study, we observed an increase in caecal butyrate after WP intervention, which may be related to the significant upregulation of *Turicibacter*. Furthermore, correlation analysis revealed a positive correlation between *Turicibacter* and ICC markers (SCF and c-Kit) associated with intestinal motility (Fig. 4B). *Helicobacter* showed a significant increase in the LOP group, while WP intervention significantly downregulated this bacterium. This finding aligns with a study by Hu et al., where they found that mulberry reduced *Helicobacter* abundance and *Helicobacter* was negatively correlated with fecal defecation [26]. Our correlation analysis also indicated a positive and negative correlation between *Helicobacter* and the first black stool time and intestinal transit rate, respectively (Fig. 4B). *Jeotgalicoccus* was found to be highly enriched in the WP group. However, there are limited reports on the association between *Jeotgalicoccus* and constipation. Our correlation analysis revealed positive correlations between *Jeotgalicoccus* and parameters related to the intestinal barrier (*Zo-1* and *Claudin-1*), the anti-inflammatory factor (IL-10), markers of intestinal peristaltic pacemaker ICC (c-Kit and SCF), and the bowel movement parameter GI.

Considering the substantial influence of WP intervention on the gut microbiota composition in Lop-induced constipation mice, we were motivated to explore the subsequent changes in gut microbiota metabolites. Recent research has shown that

higher levels of SCFAs are associated with looser stools and shorter colonic transit time [27]. Butyrate, a type of SCFA, can also affect GI motility by activating smooth muscle and myenteric neurons [28]. BCFAs, a class of metabolites derived from proteolysis, have been positively linked with colonic transit time in healthy adults [29]. In our study, in Lop-induced constipation mice, WP induced significant changes in the profile of caecal SCFAs and BCFAs. Specifically, WP intervention led to a significant increase in propionate and butyrate levels among the SCFAs, and a decrease in isobutyrate, valerate, and caproate levels among the BCFAs, compared to the LOP group. These findings suggest that WP could potentially shorten intestinal transit time.

Previous research on the molecular mechanisms of peptides for relieving constipation has been scarce and challenging to reference. To address this gap, we employed transcriptomics to conduct high-throughput gene assays, aiming to shed light on the molecular mechanisms underlying constipation relief by WP. Through KEGG enrichment analysis, we identified the calcium signaling pathways as the most significantly enriched pathway related to intestinal motility. Combined with the results of transcriptomics, it was found that WP could significantly up-regulate the *Chrm1* (CHRM1, a type of GPCR), *Itpr2*/*Itpr3* (IP3R), *Calm4*/*Calml3* (CALM) and *Slc8a3* (NCX) on the calcium signaling pathway after re-determination by RT-PCR. The proliferation of enteric neuronal progenitors in the intestine was associated with increased intestinal transit rates [30]. Among the numerous mechanisms of Ca^{2+} influx in animal cells, store-operated calcium entry (SOCE) stands out as one of the most widespread (Prakriya & Lewis, 2015). Muscarinic acetylcholine receptors (mAChRs) are present in neural progenitor cells, and their activation has been shown to promote cell proliferation and neurogenesis, likely through stimulation of SOCE [6, 31-34].

Physiologically, store-operated calcium activation is triggered by the stimulation of G-protein-coupled receptors (GPCRs) or tyrosine kinase receptors, which function through the phospholipase C (PLC)-inositol 1,4,5-trisphosphate (IP3) signaling pathway to trigger the mobilization of calcium ions (Ca^{2+}) from endoplasmic reticulum (ER) reservoirs via IP3 receptor (IP3R) calcium release channels. mAChR belong to the GPCRs superfamily. In our study, WP significantly upregulated the gene expression of *Chrm1* (a member of mAChR), *Itpr2*, and *Itpr3*. These findings indicates that WP may promote Ca^{2+} influx by activating cholinergic receptors, thereby increasing cytoplasmic Ca^{2+} levels. Intracellular Ca^{2+} can modulate the mitogen-activated protein kinase (MAPK) cascade through 2 mechanisms: calcium-dependent tyrosine kinase or CALM (one of the Ca^{2+} sensors), which come together in the Ras pathway, resulting in MAPK activation [35]. In our study, WP intervention significantly upregulated the gene expression of *Calml3* and *Calm4*, indicating a potential promotion of colonic nerve cell proliferation by WP. To test this hypothesis, we employed a 3D microscope to observe the shape of colonic nerves after clearing the colon tissue. The results revealed a significant reduction in the number of nerves in the colon tissue following Lop modeling, while WP intervention increased the number of nerves. Interestingly, glutamine (Gln), the main ingredient in WP, is known to act as a signaling molecule for intestinal cell proliferation via MAPKs. However, previous research on Gln's promotion of cell proliferation has primarily focused on its additive effects with insulin growth factor-1 or epidermal growth factor, rather than its influence on GPCRs (Rhoads & Wu, 2009). Therefore, WP's alleviating effect on constipation may be partially explained by its activation of mAChR subsequent upregulation of the calcium signaling pathway, leading to enteric neurogenesis and enhanced intestinal peristalsis ability.

5. Conclusions

The present study revealed that WP (0.5 mg/g.bw) effectively alleviated Lop-induced constipation by enhancing bowel movement function and small intestinal motility, reversing intestinal damage caused by Lop, enhancing intestinal barrier, mitigating low-grade inflammation, and balancing enteric nervous factors secretion. In terms of gut microbes, WP ameliorated constipation-associated symptoms by rectifying Lop-induced dysbiosis and promoting the growth of beneficial gut microbiota, such as the *Bifidobacterium* genus and butyrate-producing genera, which exhibit probiotic characteristics. To investigate the mechanisms underlying these improvements, we discovered that WP activated muscarinic acetylcholine receptor to upregulate the calcium signaling pathway, resulting in the proliferation of enteric neurogenesis and subsequently enhancing intestinal peristalsis ability.

Acknowledgements

This research was funded by the National Natural Science Foundation of China (32072224; 32372316; 321722141).

Declaration of Competing Interest

The authors report no declarations of interest.

References

1. A. E. Bharucha, J. H. Pemberton and G. R. Locke, III, American gastroenterological association technical review on constipation, *Gastroenterology*, 2013, **144**, 218-238.

2. D. O. Prichard and A. E. Bharucha, Recent advances in understanding and managing chronic constipation, *F1000Res*, 2018, **7**.

3. L. Chang, A. Lembo and S. Sultan, American gastroenterological association institute technical review on the pharmacological management of irritable bowel syndrome, *Gastroenterology*, 2014, **147**, 1149-+.

4. Q. Wang, F. Shen, J. Zhang, H. Cai, Y. Pan, T. Sun, Y. Gong, J. Du, H. Zhong and F. Feng, Consumption of wheat peptides improves functional constipation: a translational study in humans and mice, *Molecular Nutrition & Food Research*, 2022, DOI: 10.1002/mnfr.202200313.

5. L. Dong, Z. Xu, G. Huang, R. Zhang, M. Deng, F. Huang and D. Su, Lychee pulp-derived dietary fiber-bound phenolic complex upregulates the SCFAs-GPRs-ENS pathway and aquaporins in loperamide-induced constipated mice by reshaping gut microbiome, *Journal of Agricultural and Food Chemistry*, 2023, **71**, 15087-15096.

6. W. Q. Zhao, D. L. Alkon and W. Ma, c-Src protein tyrosine kinase activity is required for muscarinic receptor-mediated DNA synthesis and neurogenesis via ERK1/2 and c-AMP-responsive element-binding protein signaling in neural precursor cells, *Journal of Neuroscience Research*, 2003, **72**, 334-342.

7. W. Linlin, C. Mao, W. Jialiang, Y. Qiangqing, W. Gang, Z. Hao, Z. Jianxin and C. Wei, *Bifidobacterium longum* relieves constipation by regulating the intestinal barrier of mice, *Food & Function*, 2022, **13**, 5037-5049.

8. K. A. Sharkey and G. M. Mawe, The enteric nervous system, *Physiological Reviews*, 2023, **103**, 1487-1564.

9. W. A. Kunze, Y.-K. Mao, B. Wang, J. D. Huizinga, X. Ma, P. Forsythe and J. Bienenstock, *Lactobacillus reuteri* enhances excitability of colonic AH neurons by inhibiting calcium-dependent potassium channel opening, *Journal of Cellular and Molecular Medicine*, 2009, **13**, 2261-2270.

10. W. Qianqian, S. Fei, Z. Junhui, C. Haiying, P. Ya, S. Tengjia, G. Yihang, D. Juan, Z. Hao and F. Fengqin, Consumption of wheat peptides improves functional constipation: a translational study in humans and mice, *Molecular Nutrition and Food Research*, 2022, **66**, 2200313-2200313.

11. W. Qianqian, S. Fei, Z. Junhui, Z. Jiachen and F. Fengqin, Wheat peptides with different hydrolysis degree have similar relief effect in constipated mice, *Food Bioscience*, 2023, **52**, 102459-102459.
12. F. Shen, J. Zhuang, Q. Wang, J. Zhang, T. Liu, S. Ruan, J. Du, H. Zhong, M. Zhao and F. Feng, Screening of novel probiotics with intestinal peristalsis-promoting potential based on in vitro and in vivo investigations, *Food Bioscience*, 2023, **53**.
13. S. Fei, Z. Jiachen, W. Qianqian, Z. Junhui, H. Ying, M. Qiufen, Z. Mingjie, W. Jing, Z. Hao and F. Fengqin, Enhancement in the metabolic profile of sea buckthorn juice via fermentation for its better efficacy on attenuating diet-induced metabolic syndrome by targeting gut microbiota, *Food Research International*, 2022, **162**, 111948-111948.
14. J. Huang, S. Li, Q. Wang, X. Guan, L. Qian, J. Li, Y. Zheng and B. Lin, *Pediococcus pentosaceus* B49 from human colostrum ameliorates constipation in mice, *Food & Function*, 2020, **11**, 5607-5620.
15. S. Nojima, E. A. Susaki, K. Yoshida, H. Takemoto, N. Tsujimura, S. Iijima, K. Takachi, Y. Nakahara, S. Tahara, K. Ohshima, M. Kurashige, Y. Hori, N. Wada, J.-i. Ikeda, A. Kumanogoh, E. Morii and H. R. Ueda, CUBIC pathology: three-dimensional imaging for pathological diagnosis, *Scientific Reports*, 2017, **7**.
16. C. J. Streutker, J. D. Huizinga, D. K. Driman and R. H. Riddell, Interstitial cells of Cajal in health and disease. Part I: Normal ICC structure and function with associated motility disorders, *Histopathology*, 2007, **50**, 176-189.
17. X. Zhang, H. Yang, J. Zheng, N. Jiang, G. Sun, X. Bao, A. Lin and H. Liu, Chitosan oligosaccharides attenuate loperamide-induced constipation through regulation of gut microbiota in mice, *Carbohydrate Polymers*, 2021, **253**.
18. N. Li and J. Neu, Glutamine Deprivation Alters Intestinal Tight Junctions via a PI3-K/Akt Mediated Pathway in Caco-2 Cells, *Journal of Nutrition*, 2009, **139**, 710-714.
19. S. Beutheu, I. Ghouzali, L. Galas, P. Dechelotte and M. Coeffier, Glutamine and arginine improve permeability and tight junction protein expression in methotrexate-treated Caco-2 cells, *Clinical Nutrition*, 2013, **32**, 863-869.

20. M. Coeffier, O. Miralles-Barrachina, F. Le Pessot, O. Lalaude, M. Daveau, A. Lavoinne, E. Lerebours and P. Dechelotte, Influence of glutamine on cytokine production by human gut in vitro, *Cytokine*, 2001, **13**, 148-154.

21. M. Coeffier, R. Marion, P. Ducrotte and P. Dechelotte, Modulating effect of glutamine on IL-1 beta-induced cytokine production by human gut, *Clinical Nutrition*, 2003, **22**, 407-413.

22. D. A. Drossman, Functional gastrointestinal disorders: history, pathophysiology, clinical features, and Rome IV, *Gastroenterology*, 2016, **150**, 1262-+.

23. N. Prochazkova, G. Falony, L. O. Dragsted, T. R. Licht, J. Raes and H. M. Roager, Advancing human gut microbiota research by considering gut transit time, *Gut*, 2023, **72**, 180-191.

24. M. Chai, L. Wang, X. Li, J. Zhao, H. Zhang, G. Wang and W. Chen, Different *Bifidobacterium bifidum* strains change the intestinal flora composition of mice via different mechanisms to alleviate loperamide-induced constipation, *Food & Function*, 2021, **12**, 6058-6069.

25. D. Lu, Y. Pi, H. Ye, Y. Wu, Y. Bai, S. Lian, D. Han, D. Ni, X. Zou, J. Zhao, S. Zhang, B. Kemp, N. Soede and J. Wang, Consumption of dietary fiber with different physicochemical properties during late pregnancy alters the gut microbiota and relieves constipation in sow model, *Nutrients*, 2022, **14**.

26. T.-G. Hu, P. Wen, H.-Z. Fu, G.-Y. Lin, S.-T. Liao and Y.-X. Zou, Protective effect of mulberry (Morus atropurpurea) fruit against diphenoxylate-induced constipation in mice through the modulation of gut microbiota, *Food & Function*, 2019, **10**, 1513-1528.

27. J. Jones, S. N. Reinke, A. Ali, D. J. Palmer and C. T. Christophersen, Fecal sample collection methods and time of day impact microbiome composition and short chain fatty acid concentrations, *Scientific Reports*, 2021, **11**.

28. G. Haschke, H. Schafer and M. Diener, Effect of butyrate on membrane potential, ionic currents and intracellular Ca^{2+} concentration in cultured rat myenteric neurones, *Neurogastroenterology and Motility*, 2002, **14**, 133-142.

29. N. Nestel, J. D. Hvass, M. I. Bahl, L. H. Hansen, L. Krych, D. S. Nielsen, L. O. Dragsted and H. M. Roager, The Gut Microbiome and Abiotic Factors as Potential Determinants of

603 Postprandial Glucose Responses: A Single-Arm Meal Study, *Frontiers in Nutrition*, 2021,
604 **7**.
605 30. F. De Vadder, E. Grasset, L. Manneras Holm, G. Karsenty, A. J. Macpherson, L. E.
606 Olofsson and F. Backhed, Gut microbiota regulates maturation of the adult enteric
607 nervous system via enteric serotonin networks, *Proceedings of the National Academy of*
608 *Sciences of the United States of America*, 2018, **115**, 6458-6463.
609 31. P. Atluri, M. W. Fleck, Q. Shen, S. J. Mah, D. Stadfelt, W. Barnes, S. K. Goderie, S.
610 Temple and A. S. Schneider, Functional nicotinic acetylcholine receptor expression in
611 stem and progenitor cells of the early embryonic mouse cerebral cortex, *Developmental*
612 *Biology*, 2001, **240**, 143-156.
613 32. B. P. Williams, C. J. Milligan, M. Street, F. M. Hornby, J. Deuchars and N. J. Buckley,
614 Transcription of the M1 muscarinic receptor gene in neurons and neuronal progenitors of
615 the embryonic rat forebrain, *Journal of Neurochemistry*, 2004, **88**, 70-77.
616 33. R. R. Resende, K. N. Gomes, A. Adhikari, L. R. G. Britto and H. Ulrich, Mechanism of
617 acetylcholine-induced calcium signaling during neuronal differentiation of P19
618 embryonal carcinoma cells in vitro, *Cell Calcium*, 2008, **43**, 107-121.
619 34. C. Zhou, Z. X. Wen, D. M. Shi and Z. P. Xie, Muscarinic acetylcholine receptors involved
620 in the regulation of neural stem cell proliferation and differentiation in vitro, *Cell Biology*
621 *International*, 2004, **28**, 63-67.
622 35. K. Rosenblum, M. Futter, M. Jones, E. C. Hulme and T. V. P. Bliss, ERKI/II regulation by
623 the muscarinic acetylcholine receptors in neurons, *Journal of Neuroscience*, 2000, **20**,
624 977-985.
625
626

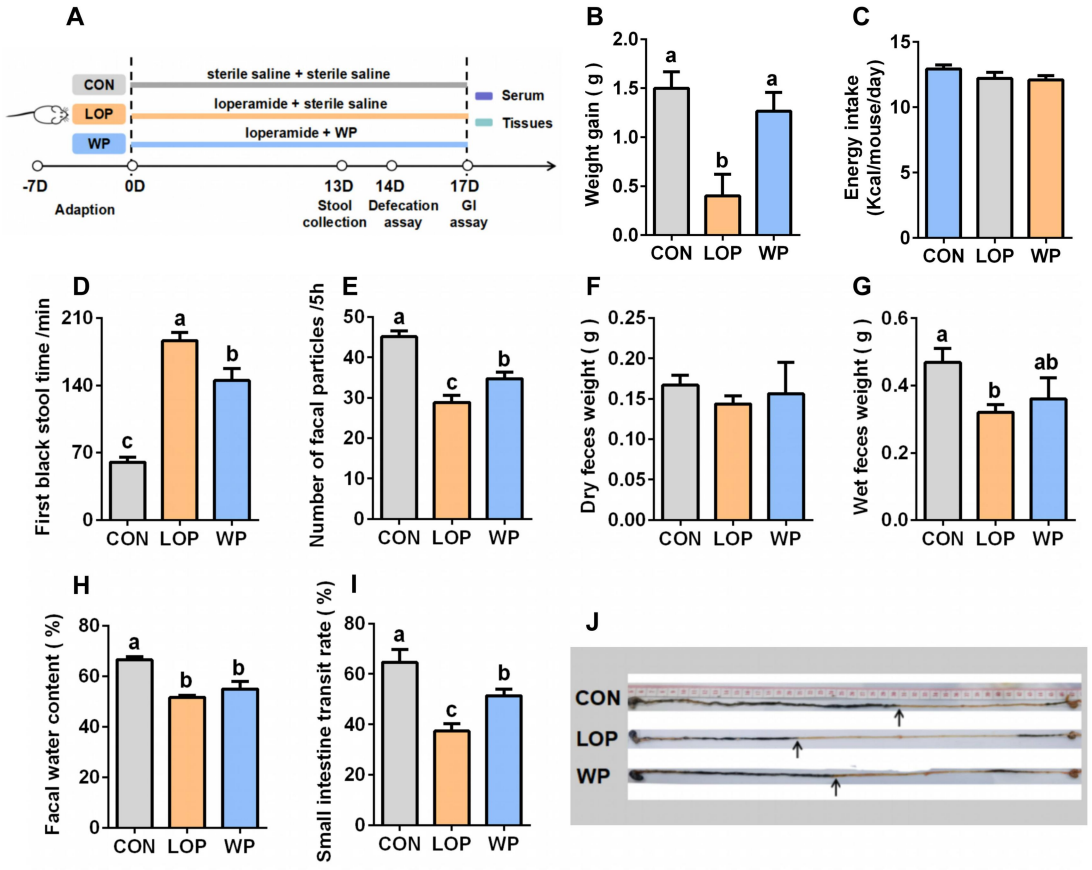


Fig. 1 Beneficial effects of WP supplementation on the defecation status of constipated mice. (A) animal experimental design, (B) body weight gain, (C) energy intake, (D) first black stool time, (E) number of fecal pellets in 5h, (F) dry feces weight, (G) wet feces weight, (H) fecal water content, (I) small intestine transit rate, (J) picture of small intestine transit. Data shown mean ± SEM (n = 12). Different letters were represented statistical significance between the groups ($P < 0.05$).

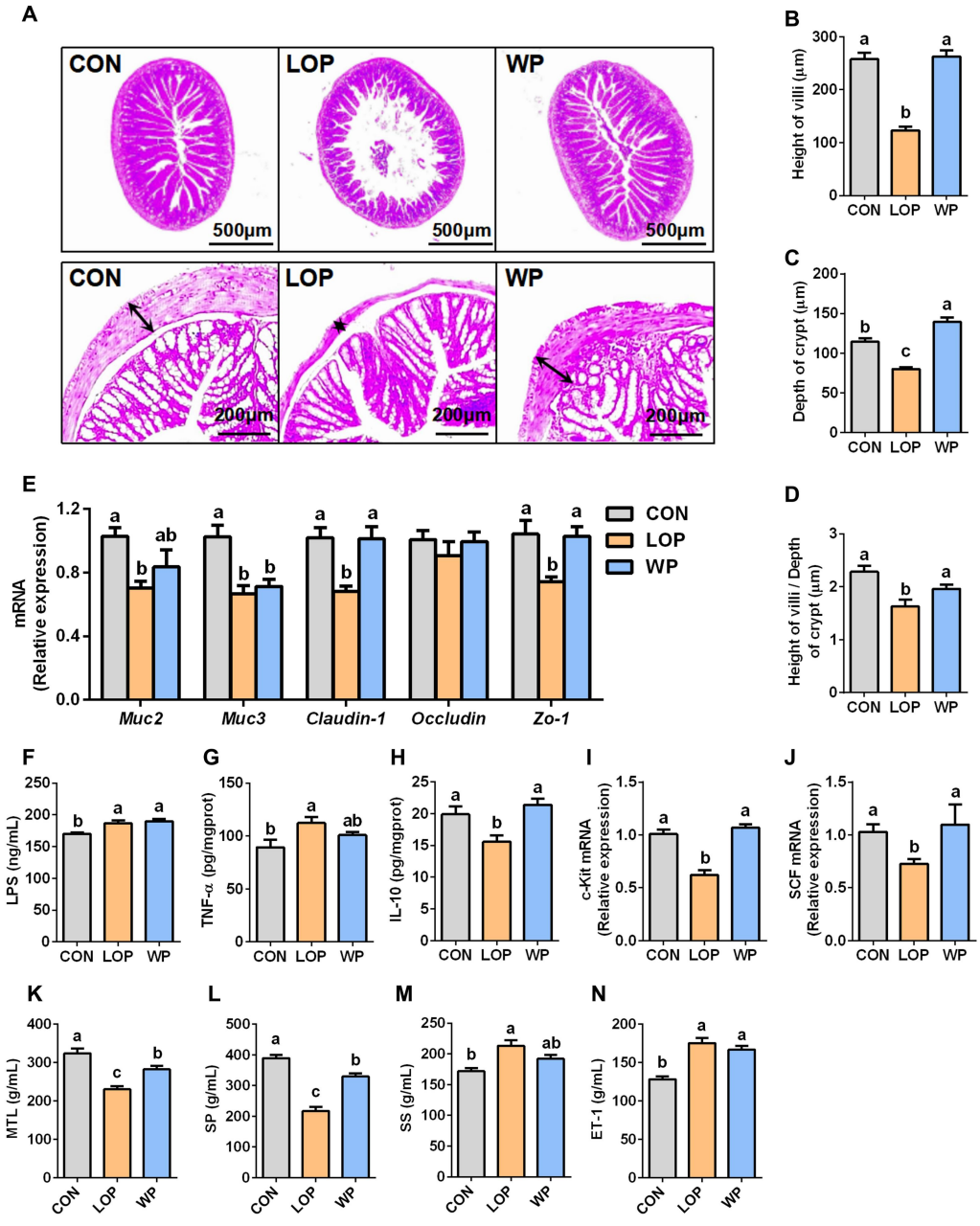
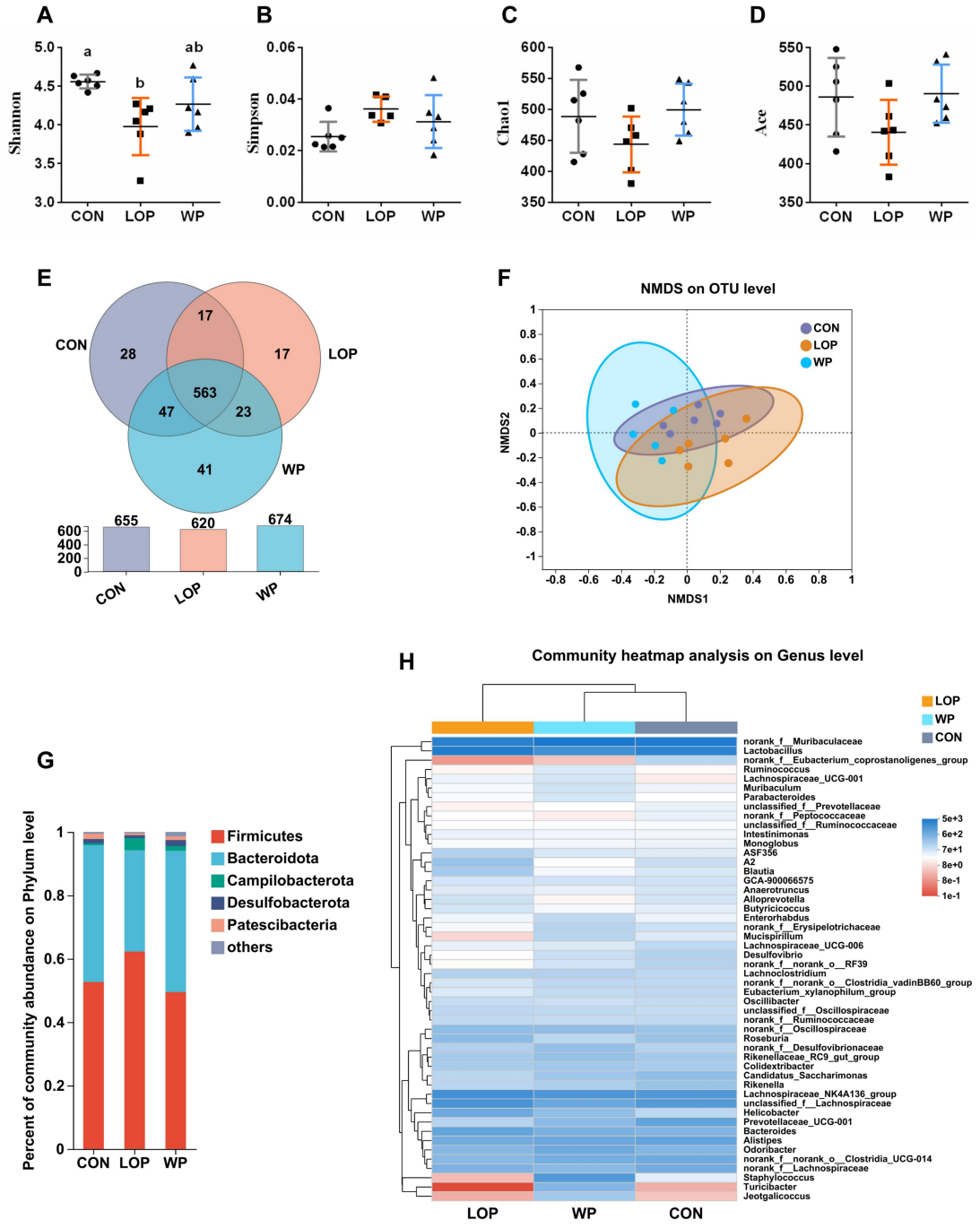


Fig. 2 WP supplementation improved the intestinal tissue damage, gut barrier, low grade inflammation, and disturbances of intestinal function and balanced the secretion of enteric nervous factors in constipated mice. (A) Histopathological analysis, (B) ileum villi height, (C) ileum crypt depth, (D) height of villi/depth of crypt, (E) transcriptional expressions of intestinal barrier in colon by RT-qPCR, (F) serum LPS, (G) TNF-α, and (H) IL-10 of colon tissue, gene I) *c-Kit*, and J) *SCF* relative expression, (K) MTL, (L) SP, (M) SS, (N) ET-1. Data shown mean ± SEM (n = 6). Different letters were represented statistical significance between the groups ($P < 0.05$).



641

642 **Fig. 3** WP supplementation recovered the structure of intestinal microbiota in constipated mice.

643 (A) Shannon index, (B) Simpson index, (C) Chao1's index, (D) Ace index, (E) OTU Venn

644 diagram, (F) β-diversity, (G) Relative abundance of gut microbiota at the phylum level, (H)

645 Community heatmap analysis on genus level. Data are expressed as mean ± SEM (n = 6).

646 Different letters were represented statistical significance between the groups ($P < 0.05$).

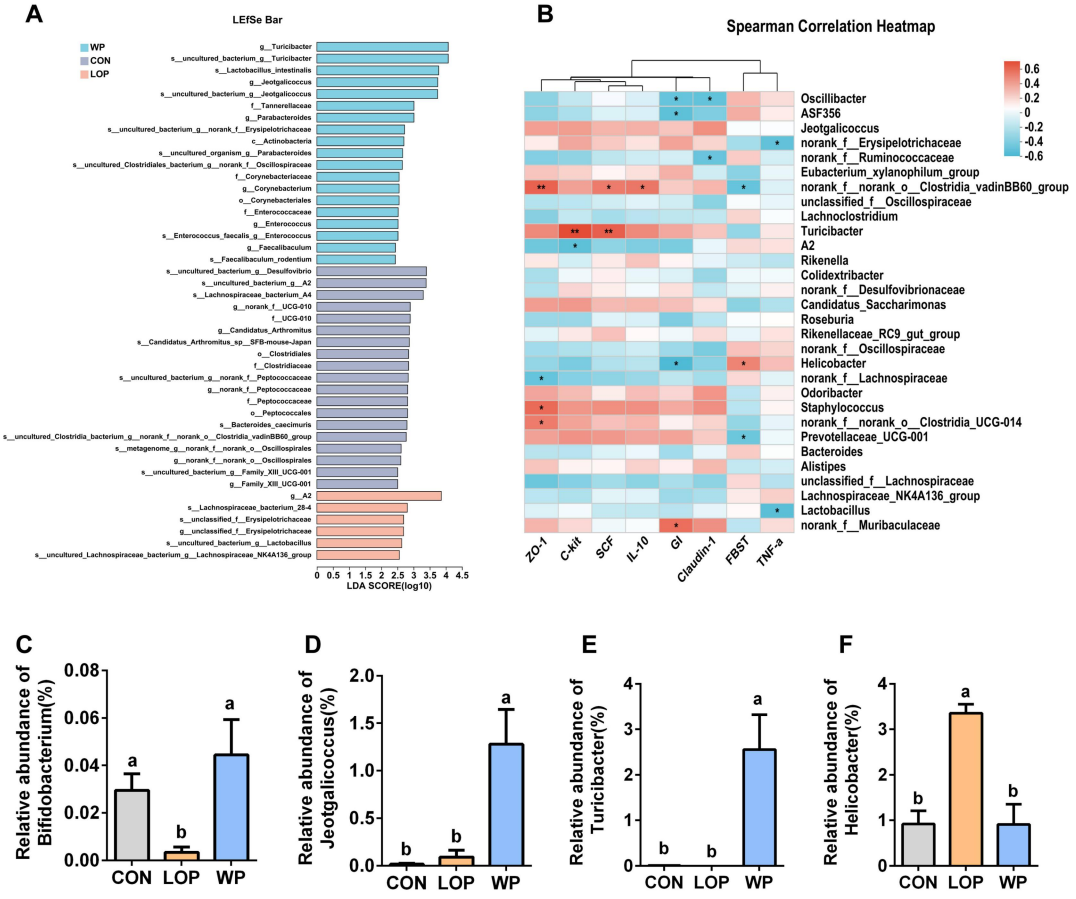
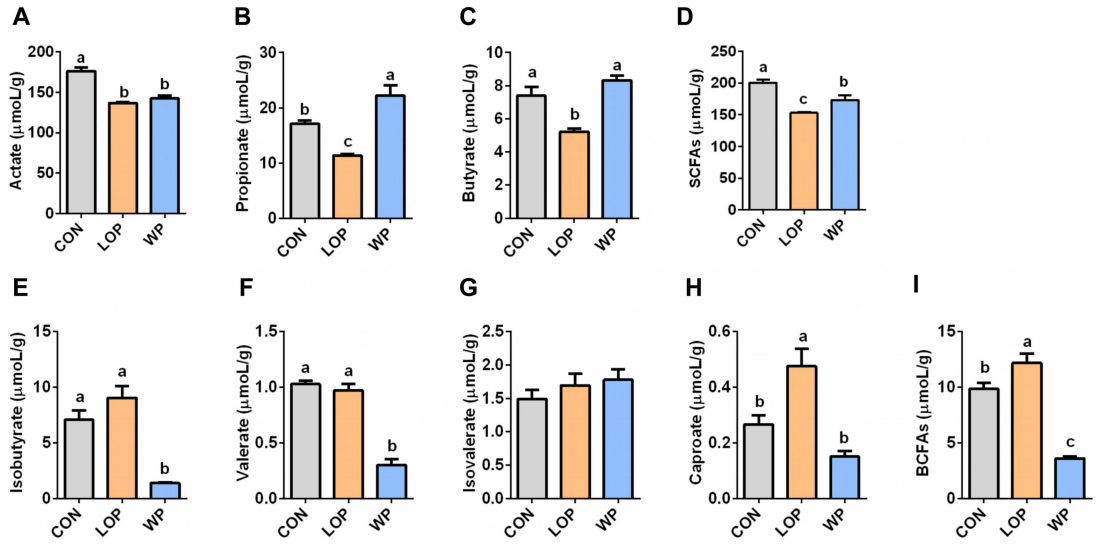


Fig. 4 WP supplementation remolded the intestinal microbiota composition. (A) LEfSe analysis, (B) correlation between gut microbiota and constipation-related indexes. The relative abundances of (C) *Bifidobacterium*, (D) *Jeotgalicoccus*, (E) *Turicibacter*, and (F) *Helicobacter*. Data are expressed as mean ± SEM (n = 6). Different letters were represented statistical significance between the groups ($P < 0.05$).



654

655 **Fig. 5** The concentrations of caeca SCFAs and BCFAs. (A) acetate content, (B) propionate

656 content, (C) butyrate content, (D) total SCFAs content, (E) isobutyrate content, (F) valerate

657 content, (G) isovalerate content, (H) caproate content, (I) total BCFAs content. Data are expressed

658 as mean ± SEM (n=8). Different letters were represented statistical significance between the

659 groups ($P < 0.05$).

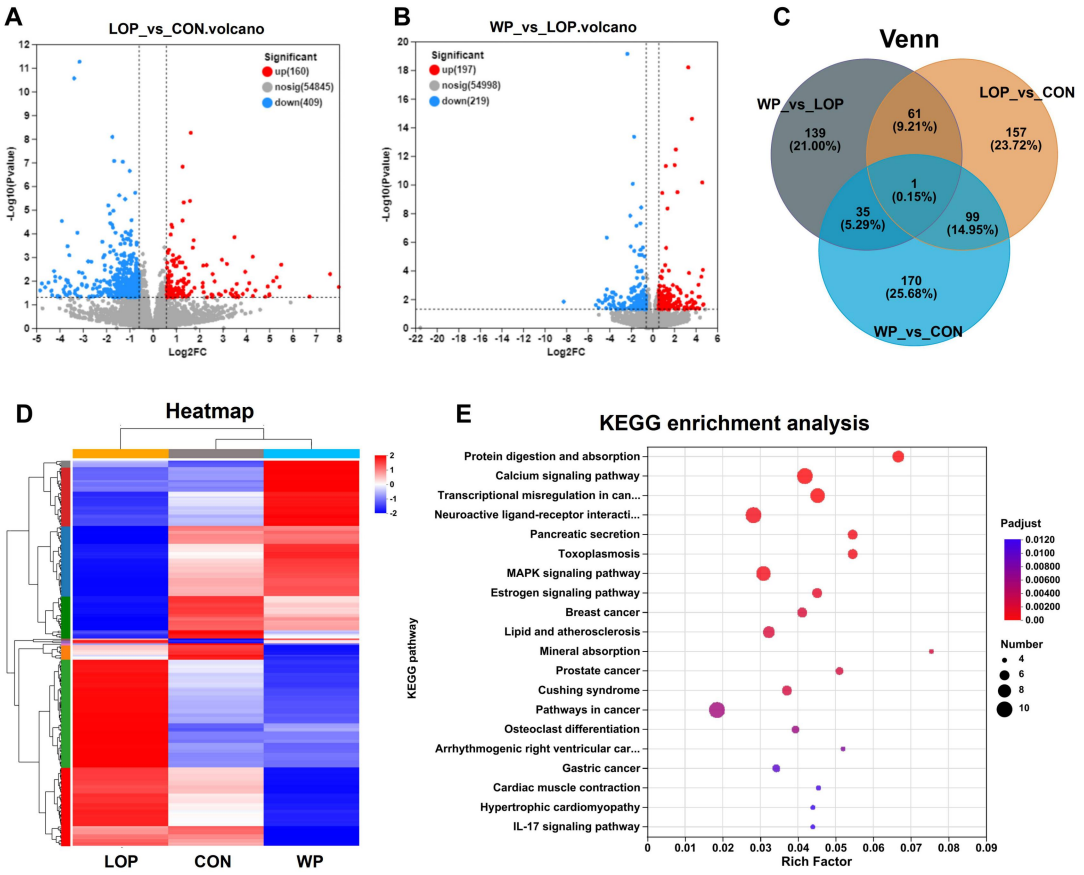
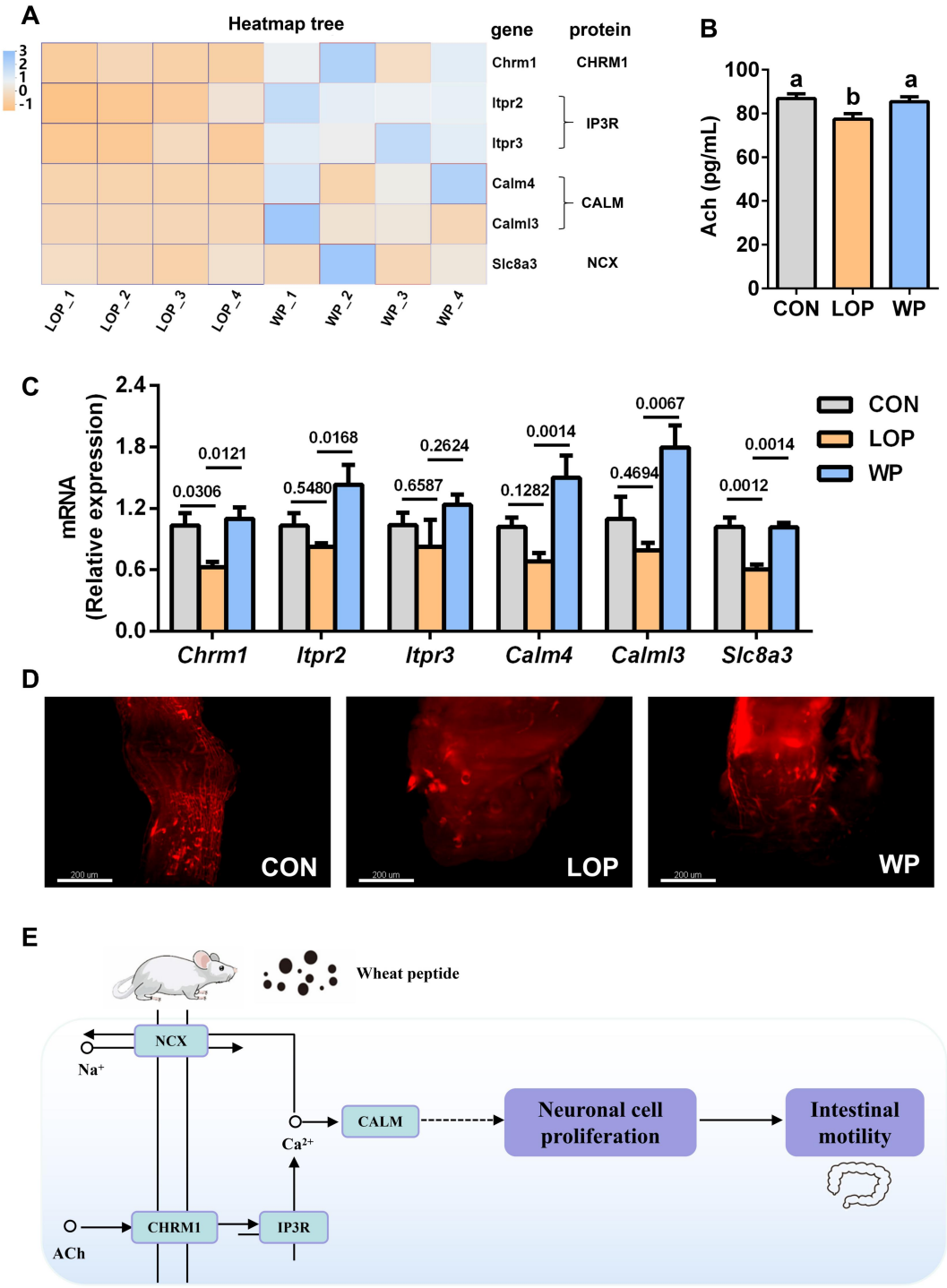


Fig. 6 Effect of WP treatment on colonic gene expression by transcriptome analysis. Volcano plots of (A) LOP group vs. CON group, and (B) WP group vs. LOP group, (C) Venn diagrams of overlapping DEGs, (D) Heatmap of lower (blue) and higher (red) DEGs expression levels. (E) Scatter diagram of signal transduction pathways of KEGG.



665

666 **Fig. 7** Effect of WP treatment on calcium signaling pathway and colonic nerve. Volcano plots of

667 (A) Heatmap tree of DEGs for calcium signaling pathway in transcriptome results (WP group vs.

668 LOP group), (B) serum Ach, (C) transcriptional expressions of *Chrm1*, *Itpr2*, *Itpr3*, *Calml4*,

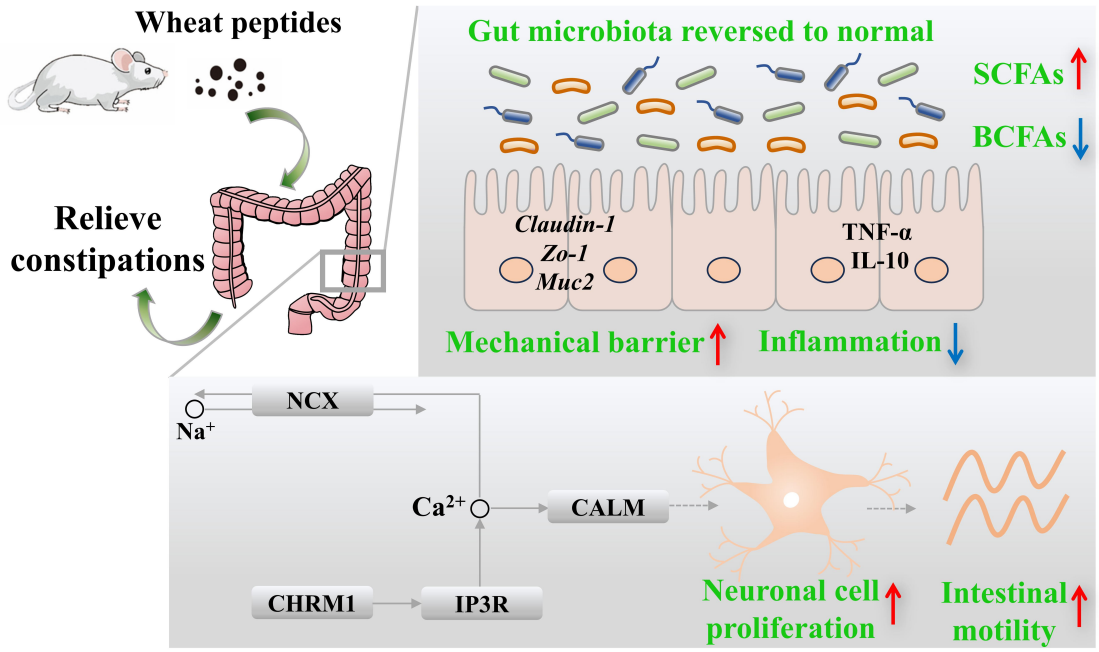
669 *Calml3*, and *Slc8a3* in colon by RT-qPCR, (D) images of the colonic nerves, (E) mechanism of

670 WP on relieving constipation in constipated mice. Data are expressed as mean ± SEM (n=6).

671 Different letters were represented statistical significance between the groups ($P < 0.05$).

672

Graphical Abstract



673

674

Supplementary material

Table S1. Sequences of primers used in the study.

Genes	Forward primer (5'-3')	Reverse primer (5'-3')
GAPDH	AGGTCGGTGTGAACGGATTTG	TGTAGACCATGTAGTTGAGGTCA
Muc2	ATGCCCACCTCCTCAAAGAC	GTAGTTTCCGTTGGAACAGTGAA
Muc3	GCCGTGAATTGTATGAACGGA	CGCAGTTGACCACGTTGACTA
Claudin-1	GGGGACAACATCGTGACCG	AGGAGTCGAAGACTTTGCACT
Occludin	TTGAAAGTCCACCTCCTTACAGA	CCGGATAAAAAGAGTACGCTGG
ZO-1	ACCACCAACCCGAGAAGAC	CAGGAGTCATGGACGCACA
c-Kit	GCCACGTCTCAGCCATCTG	GTCGCCAGCTTCAACTATTAACT
SCF	AAACTGGTGGCGAATC	CACGGGTAGCAAGAAC
Chrm1	AGTCCCAACATCACCGTCTTG	CAGGTTGCCTGTCACTGTAGC
Itpr2	CCTCGCCTACCACATCACC	TCACCACTCTCACTATGTCGT
Itpr3	GGGCGCAGAACAACGAGAT	GAAGTTTTGCAGGTCACGGTT
Calm4	ATATCAGCGTCGAGGAACTTGG	TGGTCAAGGACATTGAACACAG
Calml3	CTGACTGAGGAGCAAATCGC	TTGTCAATTTCATTCACCATGCC
Slc8a3	CCCCCGCATGGTGGATATG	CCCTCCTGCACTAACAGTGA
Cacna2d2	TGGGTGCCTATAAGGAGTACC	TTGCTGATTGGCAACTTGACC

Table S2. Changes in gene transcript patterns in calcium signaling pathway of mouse colon tissue among CON, LOP and WP groups

Gene id	Gene name	Gene description	Corresp-onding protein	LOP vs CON (log2fc)	LOP vs CON (pvalue)	WP vs LOP (log2fc)	WP vs LOP (pvalue)
ENSMUSG00000032773	*Chrm1*	Cholinergic receptor, muscarinic 1	GPCR	-1.0779	0.0488	1.4072	0.0311
ENSMUSG00000030287	*Itpr2*	Inositol 1,4,5-triphosphate receptor 2	IP3R	-0.2681	0.1549	0.9124	0.0215
ENSMUSG00000042644	*Itpr3*	Inositol 1,4,5-triphosphate receptor 3	IP3R	-0.0374	0.7955	0.8761	0.0788
ENSMUSG00000033765	*Calm4*	Calmodulin 4	CALM	-1.4016	0.0585	1.1665	0.7407
ENSMUSG00000063130	*Calml3*	calmodulin-like 3	CALM	-0.2832	0.0605	2.3113	0.5028
ENSMUSG00000079055	*Slc8a3*	Solute carrier family 8	NCX	-1.2343	0.0041	1.1706	0.0160

	(sodium/calcium exchanger), member 3

Supplementary Files

This is a list of supplementary files associated with this preprint. Click to download.

- Statement.doc